Kinetic and Mechanistic Study of the Reaction of Atomic Chlorine with Methyl Iodide over the Temperature Range 218−694 K

Y. V. Ayhens[†] and J. M. Nicovich

Georgia Tech Research Institute, Georgia Institute of Technology, Atlanta, Georgia 30332

M. L. McKee

Department of Chemistry, Auburn University, Auburn, Alabama 36849

P. H. Wine*

School of Chemistry and Biochemistry, School of Earth and Atmospheric Sciences, and Georgia Tech Research Institute, Georgia Institute of Technology, Atlanta, Georgia 30332

Received: August 18, 1997; In Final Form: September 30, 1997[⊗]

A laser flash photolysis−resonance fluorescence technique has been employed to study the kinetics of the reaction of chlorine atoms with methyl iodide as a function of temperature (218−694 K) and pressure (5−500 Torr) in nitrogen buffer gas. At $T \geq 364$ K, measured rate coefficients are pressure independent and a significant H/D kinetic isotope effect is observed, suggesting that hydrogen transfer is the dominant reaction pathway; the following Arrhenius expression adequately describes all kinetic data at 364 K $\leq T \leq$ 694 K: $k_{1a} = 5.44 \times 10^{-11} \exp(-1250/T)$ cm^3 molecule^{-1} s^{-1}. At $T \leq 250$ K, measured rate coefficients are pressure dependent and much faster than computed from the above Arrhenius expression for the H-transfer pathway, suggesting that the dominant reaction pathway at low temperature is formation of a stable adduct; at $T = 218$ K and $P = 500$ Torr, for example, $k_1 = k_{1a} + k_{1b} = 3.0 \times 10^{-11}$ cm^3 molecule^{-1} s^{-1}, with 99.4% of the reactivity being attributable to the addition channel 1b. At temperatures in the range 263−309 K, reversible addition is observed, thus allowing equilibrium constants for CH_3ICl formation and dissociation to be determined. Second- and third-law analyses of the equilibrium data lead to the following thermochemical parameters for the association reaction 1b: $\Delta H^\circ_{298} = -53.6 \pm 3.4$ kJ mol^{-1}, $\Delta H^\circ_0 = -52.2 \pm 3.5$ kJ mol^{-1}, and $\Delta S^\circ_{298} = -88 \pm 11$ J mol^{-1} K^{-1}. In conjunction with the well-known heats of formation of Cl and CH_3I, the above ΔH values lead to the following heats of formation for CH_3ICl at 298 and 0 K: $\Delta H^\circ_{f,298} = 82.3 \pm 3.5$ kJ mol^{-1} and $\Delta H_{f,0} = 91.6 \pm 3.6$ kJ mol^{-1}. Ab initio calculations using density functional theory (DFT) and G2 theory reproduce the experimental bond strength reasonably well. The DFT calculations predict a structure (used in the third-law analysis) where the C−I−Cl bond angle is 85.2° and the methyl group adopts a staggered orientation with a pronounced tilt toward chlorine. Bonding in CH_3ICl is discussed as are the implications of the new kinetic data for atmospheric chemistry.

Introduction

Methyl iodide (CH_3I) is a ubiquitous iodine-containing compound in the atmosphere; it is emitted into the atmosphere in large quantity from the oceans.[1−6] Once in the atmosphere, CH_3I and other organo-iodine compounds are rapidly photolyzed, thus initiating chain reactions involving IO_x radicals which can have important impacts on atmospheric levels of ozone and other oxidants.[6−10]

The lifetime of CH_3I toward photolysis in the atmosphere is estimated to be a few days.[11,12] The only other potential atmospheric sink for CH_3I which has received much attention is reaction with the OH radical. Laboratory studies of the OH + CH_3I reaction[13,14] suggest a rate coefficient around 10^{-13} cm^3 molecule^{-1} s^{-1} at 298 K which, given a typical atmospheric OH concentration of 10^6 molecules cm^{-3},[15] leads to the conclusion that this reaction is of only minor importance as a CH_3I sink.

Until recently, it has been thought that chlorine atom levels in the troposphere were so low that Cl could not be an important tropospheric reactant. However, evidence is now mounting which suggests that chlorine atom levels in the marine boundary layer (where most CH_3I enters the atmosphere) may be as much as one-tenth as high as OH levels,[16−19] with the chlorine atom source probably being photochemically labile chlorine species such as Cl_2 and $ClNO_2$ produced via heterogeneous reactions on the surfaces of moist sea salt particles.[20] Since chlorine atom reactions with many organics are considerably faster than the corresponding OH reaction, it is possible that reaction with Cl could be a nonnegligible sink for atmospheric CH_3I. Although numerous kinetics studies of Cl reactions with CH_3F,[21−24] CH_3Cl,[21,22,25,26] and CH_3Br[27,28] have been reported in the literature, there had been no previous studies of reaction 1 at the time this research was undertaken.

$$Cl + CH_3I \rightarrow \text{products} \qquad (1)$$

However, one experimental[29] and one theoretical[30] study of reaction 1 have appeared in the literature after the results discussed in this paper were presented at a scientific meeting.[31]

* To whom correspondence should be addressed.

[†] Present address: Department of Chemistry and Biochemistry, University of Colorado, Boulder, CO 80309.

[⊗] Abstract published in *Advance ACS Abstracts,* November 15, 1997.

S1089-5639(97)02709-6 CCC: $14.00

The above-mentioned laboratory studies of Cl + CH_3X kinetics (X = F, Cl, Br) demonstrate that all three reactions proceed predominantly by hydrogen abstraction, that all three reactions have 298 K rate coefficients in the range (3−5) × 10^{-13} cm^3 $molecule^{-1}$ s^{-1}, and that all three reactions have positive activation energies in the range 8.9−10.5 kJ mol^{-1}. To be an important atmospheric process, reaction 1 would have to be much faster than the other Cl + CH_3X reactions.

In this paper we report the results of experiments where laser flash photolysis of $Cl_2/CH_3I/N_2$ mixtures has been coupled with Cl detection by time-resolved atomic resonance fluorescence spectroscopy to investigate the kinetics of reaction 1 as a function of temperature and pressure. We find that Cl reacts with CH_3I not only by hydrogen abstraction but also by (reversible) addition. At temperatures and pressures relevant for atmospheric chemistry considerations, the rate coefficient for addition is much faster than the rate coefficient for hydrogen abstraction.

Experimental Technique

Chlorine atom kinetics in the presence of varying amounts of CH_3I were studied using the laser flash photolysis (LFP)−resonance fluorescence (RF) technique. The LFP−RF apparatus was similar to those employed in several previous studies of chlorine atom kinetics.[32−34] Important features of the apparatus and experimental techniques which are specific to this study are described below.

Two different reaction cells were employed in this study. All experiments at subambient temperatures and some experiments at 295 K < T < 450 K employed a jacketed Pyrex reaction cell with an internal volume of approximately 160 cm^3. The cell was maintained at a constant temperature by circulating ethylene glycol (for T > 295 K) or a 2:1 ethanol−methanol mixture (for T < 295 K) from a thermostated bath through the outer jacket. All experiments at T > 450 K and some experiments at 295 K < T < 450 K employed a quartz reaction cell with an internal volume of approximately 250 cm^3. The cell was maintained at a constant temperature by passing a well-controlled electrical current through high-resistance-wire heaters which were wrapped around the cell. Copper−constantan (for low-temperature studies) or chromel−alumel (for high-temperature studies) thermocouples could be injected into the reaction zone through a vacuum seal, thus allowing measurement of the gas temperature under the precise pressure and flow rate conditions of the experiment. Temperature variation within the reaction volume, i.e., the volume from which fluorescence could be detected, was found to be ≤1 K at T ∼ 160 K and ≤2 K at T ∼ 700 K.

Chlorine atoms were produced by 355 nm laser flash photolysis of Cl_2. Third harmonic radiation from a Quanta Ray Model DCR-2 Nd:YAG laser provided the photolytic light source. The photolysis laser could deliver up to 1 × 10^{17} photons per (6 ns) pulse at a repetition rate of up to 10 Hz. Fluences employed in this study ranged from 10 to 150 mJ cm^{-2} $pulse^{-1}$.

To avoid accumulation of photochemically generated reactive species, all experiments were carried out under "slow flow" conditions. The linear flow rate through the reactor was typically 2.5 cm s^{-1}, while the laser repetition rate was varied over the range 5−10 Hz (it was 10 Hz in most experiments). Since the direction of flow was perpendicular to the photolysis laser beam, no volume element of the reaction mixture was subjected to more than a few laser shots. Molecular chlorine (Cl_2), $CH_3I(CD_3I)$, and CF_2Cl_2 flowed into the reaction cell from 12 L Pyrex bulbs containing mixtures in nitrogen buffer gas, while N_2 flowed directly from its high-pressure storage tank; the bulb containing $CH_3I(CD_3I)$ was blackened to prevent photolysis by room lights. The gas mixtures and additional N_2 were premixed before entering the reaction cell. Concentrations of each component in the reaction mixture were determined from measurements of the appropriate mass flow rates and the total pressure. In addition, the fraction of $CH_3I(CD_3I)$ in the $CH_3I(CD_3I)/N_2$ mixture was checked frequently by UV photometry at 254 nm using a mercury penray lamp as the light source. The absorption cross section needed to convert measured absorbances to concentrations was measured during the course of this study; in units of 10^{-19} cm^2 $molecule^{-1}$ (base e) the absorption cross sections were found to be 11.6 for CH_3I and 11.9 for CD_3I; for CH_3I, the agreement with literature values is good.[11,12,35] In experiments where relatively high CH_3I (CD_3I) concentrations were employed, the CH_3I (CD_3I) concentration was measured in situ in the slow flow system using a 2-m long absorption cell; measured rate coefficients were independent of the absorption cell position in the flow system, i.e., upstream or downstream from the reaction cell.

The gases used in this study had the following stated minimum purities: N_2, 99.999%; Cl_2, 99.9%;[36] CF_2Cl_2, 99.9%.[36] Nitrogen was used as supplied while Cl_2 and CF_2Cl_2 were degassed at 77 K before being used to prepare mixtures with N_2. The liquid CH_3I sample had a stated purity of 99%, while the isotopic purity of the CD_3I was greater than 99.5%. CH_3I and CD_3I were transferred under nitrogen atmosphere into a vial fitted with a high-vacuum stopcock and then degassed repeatedly at 77 K before being used to prepare mixtures with N_2.

Results and Discussion

In all LFP−RF experiments, chlorine atoms were generated by laser flash photolysis of Cl_2 at 355 nm:

$$Cl_2 + h\nu(355\ nm) \rightarrow nCl(^2P_{3/2}) + (2-n)Cl(^2P_{1/2}) \quad (2)$$

The fraction of chlorine atoms generated in the excited spin−orbit state, $Cl(^2P_{1/2})$, is thought to be very small, i.e., less than 0.01.[37,38] Recently, it has been reported that the rate coefficient for $Cl(^2P_{1/2})$ quenching by N_2 is slower than previously thought, i.e., 5.0 × 10^{-15} cm^3 $molecule^{-1}$ s^{-1}.[39] However, on the basis of reported rate coefficients for $Cl(^2P_{1/2})$ deactivation by saturated halocarbons (all gas kinetic except CF_4),[39−42] we expect that the rate coefficient for $Cl(^2P_{1/2})$ deactivation by CH_3I is very fast, i.e., faster than the observed Cl + CH_3I reaction rate. Hence, it seems safe to assume that all Cl + CH_3I kinetic data are representative of an equilibrium mixture of $Cl(^2P_{1/2})$ and $Cl(^2P_{3/2})$. As a further check on the assumption of spin state equilibration, some rate coefficients were measured with and without CF_2Cl_2, a very efficient $Cl(^2P_{1/2})$ quencher,[39,40,42] added to the reaction mixture; as expected, this variation in experimental conditions had no effect on the observed reaction rate.

All LFP−RF experiments were carried out under pseudo-first-order conditions with CH_3I in large excess over Cl. Hence, in the absence of side reactions that remove or produce chlorine atoms, the Cl temporal profile following the laser flash would be described by the relationship

$$\ln\{[Cl]_0/[Cl]_t\} = (k_1[CH_3I] + k_3)t = k't \quad (I)$$

where k_3 is the rate coefficient for the reaction

Cl → first-order loss by diffusion from the detector field of view and/or reaction with background impurities (3)

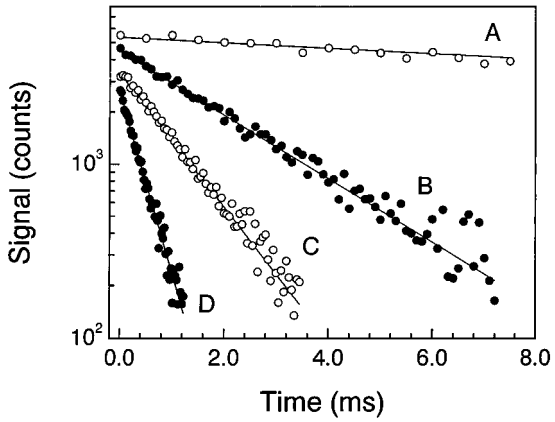

Figure 1. Typical Cl atom temporal profiles observed at $T \geq 364$ K (and at $T \leq 250$ K). Experimental conditions: $T = 532$ K; $P = 100$ Torr; $[Cl_2]$ in units of 10^{12} molecules cm^{-3} = (A) 4.1, (B) 2.1, (C) 4.1, (D) 4.1; $[Cl]_0$ in units of 10^{10} atoms cm^{-3} = (A) 6, (B) 3, (C) 6, (D) 6; $[CH_3I]$ in units of 10^{14} molecules cm^{-3} = (A) 0, (B) 0.740, (C) 1.64, (D) 4.70; number of laser shots averaged = (A) 300, (B) 4500, (C) 4000, and (D) 14 500. Solid lines are obtained from least-squares analyses and give the following pseudo-first-order decay rates in units of s^{-1}: (A) 37, (B) 418, (C) 887, (D) 2410. For the sake of clarity, traces A and D are scaled by factors of 2.2 and 0.7, respectively.

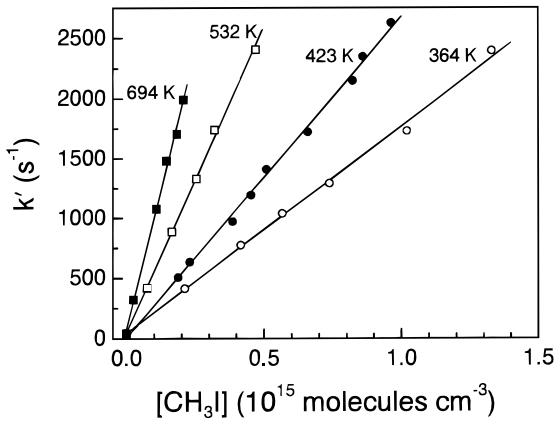

Figure 2. Plots of k', the Cl atom pseudo-first-order decay rate, versus CH_3I concentration for data at four temperatures over the range 364−694 K. All data shown were obtained at a pressure of 100 Torr. The solid lines are obtained from linear least-squares analyses, and the resulting rate coefficients, i.e., the slopes of the plots, are listed in Table 1.

The bimolecular rate coefficients of interest, $k_1(P,T)$, are determined from the slopes of k' vs $[CH_3I]$ plots for data obtained at constant P and T. Observance of Cl temporal profiles that are exponential, i.e., obey eq I, a linear dependence of k' on $[CH_3I]$, and invariance of k' to variation in laser photon fluence and photolyte concentration strongly suggest that reactions 1 and 3 are, indeed, the only processes that significantly affect the Cl time history.

Kinetics at $T \geq 364$ K. For all experiments carried out at temperatures of 364 K and above, well-behaved pseudo-first-order kinetics were observed, i.e., Cl atom temporal profiles obeyed eq I and k' increased linearly with increasing $[CH_3I]$ but were independent of laser photon fluence and photolyte concentration. Typical data are shown in Figures 1 and 2, while measured bimolecular rate coefficients, $k_1(P,T)$ and $k_4(P,T)$, are summarized in Table 1.

$$Cl + CD_3I \rightarrow \text{products} \qquad (4)$$

At 423−424 K, k_1 is found to be independent of pressure. An Arrhenius plot for reaction 1 is shown in Figure 3. A linear least-squares analysis of the ln k_1 vs l/T data gives the following Arrhenius expression (for 364 K $\leq T \leq$ 694 K):

$$k_1(T) = (5.44 \pm 1.17) \times 10^{-11} \exp[-(1250 \pm 100)/T] \text{ cm}^3 \text{ molecule}^{-1} \text{ s}^{-1}$$

Errors in the above expression are 2σ and represent precision only. Comparison of k_1 values calculated from the above Arrhenius expression with measured values of k_4 (see Table 1) shows a significant H/D kinetic isotope effect, i.e., $k_1/k_4 = 4.3$ at 373 K and $k_1/k_4 = 3.6$ at 419 K. The observed kinetic isotope effect strongly supports hydrogen transfer as the dominant reaction mechanism, while observed temperature and pressure dependencies of k_1 and k_4 are consistent with a hydrogen transfer mechanism. We conclude that, at temperatures in the range 360−700 K, the dominant channel for reaction 1 is

$$Cl + CH_3I \rightarrow CH_2I + HCl \qquad (1a)$$

Kinetics at $T \leq 250$ K. As was the case in the high-temperature experiments (see above), well-behaved pseudo-first-order kinetics were observed in all experiments at $T \leq 250$ K. However, unlike the high-temperature results, the bimolecular rate coefficients measured at $T \leq 250$ K were found to increase with increasing pressure; typical data are shown in Figure 4 and measured rate coefficients are summarized in Table 2. Comparison of the rate coefficients in Table 2 with values of k_{1a} obtained by extrapolation of the high-temperature results to $T \leq 250$ K demonstrates that the branching ratio for hydrogen transfer is very small under the temperature and pressure conditions used to obtain the data in Table 2, ranging from 0.11 at $T = 250$ K, $P = 10$ Torr to 0.0058 at $T = 218$ K, $P = 500$ Torr. The dominant reaction channel at $T \leq 250$ K and $P \geq 5$ Torr appears to be formation of a stable adduct:

$$Cl + CH_3I + M \rightarrow CH_3ICl + M \qquad (1b)$$

To describe the pressure dependence of the bimolecular rate coefficient for an association reaction at a specified temperature and for a specified bath gas, an equation of the following form is frequently employed:[43]

$$k([M],T) = k_0 k_\infty [M] F_c^X/(k_\infty + k_0[M]) \qquad \text{(II)}$$

$$X = \{1 + [\log(k_0[M]/k_\infty)]^2\}^{-1} \qquad \text{(III)}$$

In the above equations k_0 and k_∞ are approximations to the low- and high-pressure limit rate coefficients, respectively, and F_c is the "broadening parameter;" k_0 and F_c depend on both temperature and the identity of the bath gas while k_∞ depends only on temperature. Using the above parametrization to fit the kinetic date for reaction 1b at $T = 218$ K (see Table 2) gives the following results:

$$k_{1b,0}(N_2, 218 \text{ K}) = 2.0 \times 10^{-29} \text{ cm}^6 \text{ molecule}^{-2} \text{ s}^{-1}$$

$$k_{1b,\infty}(218 \text{ K}) = 4.0 \times 10^{-11} \text{ cm}^3 \text{ molecule}^{-1} \text{ s}^{-1}$$

$$F_c(N_2, 218 \text{ K}) = 0.63$$

The parametrization represents the experimental data quite well. However, it should be kept in mind that use of the above parametrization to extrapolate outside the pressure range where data are available is not recommended, i.e., a more detailed theoretical analysis is required to meet that objective.

Kinetics at 263 K $\leq T \leq$ 309 K. Over the intermediate temperature range 263−309 K, chlorine atom regeneration via

TABLE 1: Summary of Kinetic Data for the Reactions of Cl with CH_3I and CD_3I Obtained at $T \geq 364$ K[a]

CX_3I	T	P	$[Cl_2]$	$[Cl]_{t=0}$	no. of expts[b]	$[CX_3I]_{max}$	k'_{max}	$k_i \pm 2\sigma^{c,d}$
CH_3I	364	100	28	1.1	7	13300	2400	1.73 ± 0.08
	396	100	58−110	0.8−2.0	12	8740	2260	2.65 ± 0.12[e]
	399	100	96−250	1.2	7	10700	2690	2.42 ± 0.20
	423	100	25−76	0.7−2.2	10	8590	2350	2.67 ± 0.10
	424	25	37	1.1	5	14400	4140	2.75 ± 0.11
	522	100	130−310	1.1−1.7	7	5500	2720	4.62 ± 0.44
	532	100	21−41	0.3−0.6	6	4700	2410	5.10 ± 0.20
	690	100	20−82	0.4−1.1	15	2210	2050	9.20 ± 0.49
	694	100	38−72	0.6−1.1	6	2060	1990	9.30 ± 0.53
CD_3I	373	100	17	1.1	6	3580	1670	0.441 ± 0.033
	419	100	20	1.6	6	2710	2710	0.755 ± 0.014

[a] Units: T(K); P(Torr); concentrations(10^{11} cm^{-3}); k'(s^{-1}); k_i(10^{-12} cm^3 molecule^{-1} s^{-1}). [b] expt ≡ measurements of single pseudo-first-order $Cl(^2P_J)$ decay rate. [c] Errors represent precision only. [d] For CH_3I reactant, $i = 1$, while for CD_3I reactant, $i = 4$. [e] Results include some experiments with 1.1×10^{15} CF_2Cl_2 per cm^3 added as an additional $Cl(^2P_{1/2})$ quencher.

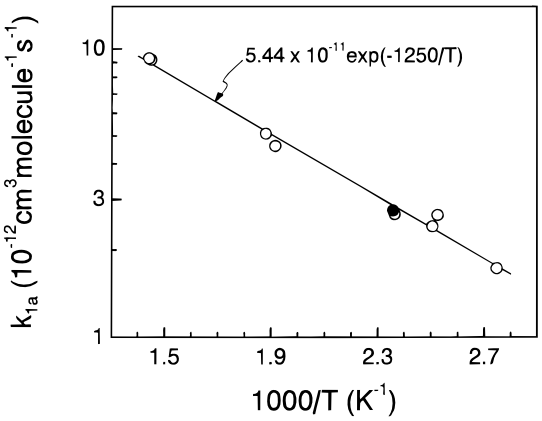

Figure 3. Arrhenius plot for the reaction $Cl + CH_3I \rightarrow CH_2I + HCl$. The filled data point was obtained at $P = 25$ Torr while all open data points were obtained at $P = 100$ Torr. The solid line is obtained from a least-squares analysis which yields the Arrhenius expression shown in the figure (units are cm^3 molecule^{-1} s^{-1}).

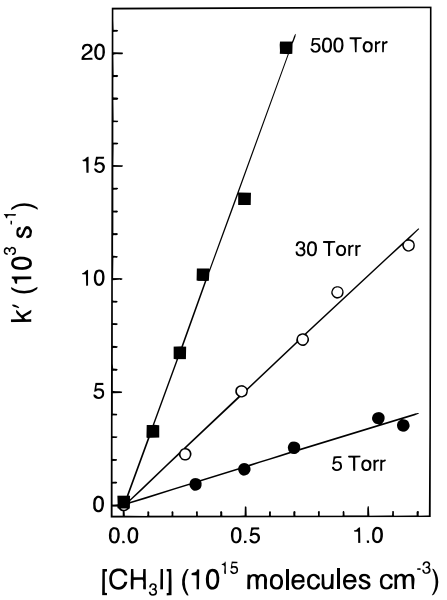

Figure 4. Plots of k', the Cl atom pseudo-first-order decay rate, versus CH_3I concentration as a function of pressure for data obtained at $T = 218$ K. The solid lines are obtained from linear least-squares analyses, and the resulting rate coefficients, i.e., the slopes of the plots, are listed in Table 2.

a secondary reaction became evident. Under these experimental conditions, observed Cl atom temporal profiles were independent of laser fluence and Cl_2 concentration but varied as a function of CH_3I concentration, pressure, and temperature in the manner expected if unimolecular decomposition of CH_3ICl was the source of regenerated chlorine atoms. As expected if Cl kinetics are controlled by adduct formation and dissociation, room temperature experiments using CD_3I as the reactant gave results which were indistinguishable from those obtained at the same pressure using CH_3I as the reactant. Assuming that CH_3ICl decomposition is the source of regenerated Cl atoms, the relevant kinetic scheme controlling the Cl temporal profile includes not only reactions 1a, 1b, and 3, but also reactions −1b and 5:

$$CH_3ICl + M \rightarrow Cl + CH_3I + M \qquad (-1b)$$

$$CH_3ICl \rightarrow \text{first order loss by processes that do not regenerate Cl atoms} \qquad (5)$$

Assuming that all processes affecting the temporal evolution of Cl and CH_3ICl are first-order or pseudo-first order, the rate equations for the above reaction scheme can be solved analytically

$$S_t/S_0 = \{(Q + \lambda_1)\exp(\lambda_1 t) - (Q + \lambda_2)\exp(\lambda_2 t)\}/(\lambda_1 - \lambda_2) \qquad (IV)$$

where S_t and S_0 are the resonance fluorescence signal levels at times t and 0, and

$$Q = k_{-1b} + k_5 \qquad (V)$$

$$Q + k_3 + (k_{1a} + k_{1b})[CH_3I] = -(\lambda_1 + \lambda_2) \qquad (VI)$$

$$Q(k_3 + k_{1a}[CH_3I]) + k_5 k_{1b}[CH_3I] = \lambda_1\lambda_2 \qquad (VII)$$

Observed Cl atom temporal profiles were fit to the double-exponential eq IV using a nonlinear least-squares method to obtain values for λ_1, λ_2, Q, and S_0. The background Cl loss rate in the absence of CH_3I, i.e., k_3, was directly measured at each temperature and pressure, and rate coefficients for the hydrogen transfer channel, i.e., k_{1a}, were obtained by extrapolation of the high-temperature kinetic data assuming Arrhenius behavior, i.e., a linear ln k_{1a} vs $1/T$ dependence from 364 K down to 263 K. Rearrangement of the above equations shows that the rate coefficients k_{1b}, k_{-1b}, and k_5 can be obtained from the fit parameters (and the experimental values for k_3 and k_{1a}) using the following equations:

$$k_{1b} = -(Q + k_3 + k_{1a}[CH_3I] + \lambda_1 + \lambda_2)/[CH_3I] \qquad (VIII)$$

$$k_5 = \{\lambda_1\lambda_2 - Q(k_3 + k_{1a}[CH_3I])\}/(k_{1b}[CH_3I]) \qquad (IX)$$

$$k_{-1b} = Q - k_5 \qquad (X)$$

TABLE 2: Summary of Kinetic Data for the Reaction of Cl with CH_3I Obtained at $T \leq 250$ K[a]

T	P	$[Cl_2]$	$[Cl]_{t=0}$	no. of expts[b]	$[CH_3I]_{max}$	$k'_{1a\ max}$	$(k' - k'_{1a})_{max}$	$k_{1b} \pm 2\sigma$[c]
218	5.1	45	1.1	6	11400	198	3490	3.31 ± 0.52
	10	48	1.1	5	9820	171	5010	5.04 ± 0.26
	30	44	1.0	6	11600	202	11500	10.2 ± 0.7
	100	57	1.4	6	9830	171	20100	19.8 ± 1.9
	250	67−140	1.6−3.3	8	7220	126	17800	25.0 ± 1.3
	500	120	3.6	6	6620	115	20200	29.7 ± 2.6
250	10	76	1.9	5	9900	360	3220	3.25 ± 0.21
	100	51	1.0	5	8300	302	11900	14.3 ± 0.7
	500	110	3.0	6	3560	129	9120	24.5 ± 1.9

[a] Units: T(K); P(Torr); concentrations(10^{11} cm^{-3}); k'_{1a}, k'(s^{-1}); k_{1b}(10^{12} cm^3 molecule^{-1} s^{-1}). [b] expt ≡ measurements of single pseudo-first-order $Cl(^2P_J)$ decay rate. [c] Errors represent precision only.

Typical chlorine atom temporal profiles observed in the experiments at $T = 263-309$ K are shown in Figure 5 along with the best fits of each temporal profile to eq IV; the results for all experiments in this temperature range are summarized in Table 3. It is worth noting that values for $k_{1b}(P,T)$ obtained from analysis of the double exponential decays observed at 263 K $\leq T \leq$ 309 K are consistent with those expected based on extrapolation of the results from lower temperatures. We believe that reported values for k_{-1b}, even at high temperatures (∼300 K) where Cl regeneration is relatively fast, are accurate to within ± 20%. Absolute uncertainties in reported values for k_{-1b} are somewhat more difficult to assess. Inspection of Table 3 shows that the precision of multiple determinations of k_{-1b} at a particular temperature and pressure (for varying CH_3I concentration) is quite good. An inherent assumption in our analysis is that the only significant CH_3ICl loss process that results in chlorine atom production is reaction −1b; as long as this assumption is correct (it almost certainly is), we estimate that the absolute accuracy of reported k_{-1b} values is ±30% over the full range of temperature and pressure spanned by the results given in Table 3.

Possible Secondary Chemistry Complications. The photochemical system used to study the kinetics of reactions 1a, 1b, and −1b appears to be relatively free of complications from unwanted side reactions. The only potential secondary reactions we are aware of which could destroy or regenerate chlorine atoms (other than reaction −1b, of course) are the following:

$$Cl + CH_2I \rightarrow \text{products} \quad (6)$$

$$Cl + CH_3ICl \rightarrow \text{products} \quad (7)$$

$$CH_2I + Cl_2 \rightarrow CH_2ICl + Cl \quad (8)$$

The concentrations of photochemically generated radicals employed in this study, i.e., $\leq 3 \times 10^{11}$ per cm^3 (see Tables 1−3), were sufficiently small that radical−radical interactions such as reactions 6 and 7 could not be important chlorine atom removal processes even if their rate coefficients were gas kinetic. Experimentally, the fact that observed kinetics were unaffected by factors of 2−3 variation in $[Cl]_0$ confirms that reactions 6 and 7 did not contribute significantly to chlorine atom removal. The kinetics of reaction 8 have been studied by Seetula et al. over the temperature range 295−524 K;[44] these authors report the Arrhenius expression $k_8 = 1.15 \times 10^{-12} \exp(-96/T)$ cm^3 molecule^{-1} s^{-1}. Since Cl_2 concentrations were less than 10^{13} per cm^3 in a large majority of experiments (see Tables 1−3), reaction 8 is not expected to be an important source of regenerated Cl under the experimental conditions employed. The interference from reaction 8 is expected to be greatest at the highest temperatures studied because k_8 increases slightly with increasing temperature and because CH_2I is produced from reaction 1 with unit yield at high temperature. At $T = 690$ K, a factor of 4 variation in Cl_2 concentration had no effect on observed kinetics, thus confirming that reaction 8 was not an important interference.

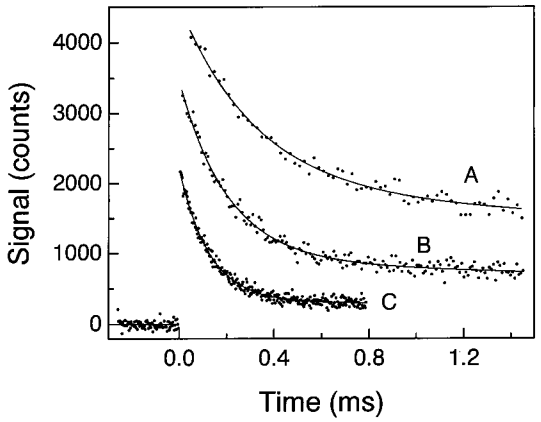

Figure 5. Typical Cl atom temporal profiles observed at 263 K $\leq T \leq$ 309 K. Experimental conditions: $T = 283$ K; $P = 100$ Torr; $[Cl_2] = 3.4 \times 10^{12}$ molecules cm^{-3}; $[Cl]_0 = 1.0 \times 10^{11}$ atoms cm^{-3}; $[CH_3I]$ in units of 10^{14} molecules cm^{-3} = (A) 1.73, (B) 3.57, (C) 6.58; number of laser shots averaged = (A) 3000, (B) 5000, (C) 13 000. Solid lines are obtained from nonlinear least-squares fits to eq II. Best fit parameters, i.e., λ_1, λ_2, and Q, are summarized in Table 3. For the sake of clarity, trace B is scaled by a factor of 1.2.

CH_3ICl Thermochemistry: Second-Law Analysis. The equilibrium constants, K_p, given in Table 3 are computed from the relationship

$$K_p = k_{1b}/(k_{-1b}RT) = K_c/RT \quad (XI)$$

A plot of ln K_p vs l/T, i.e., a van't Hoff plot, is shown in Figure 6. Since

$$\ln K_p = (\Delta S/R) - (\Delta H/RT) \quad (XII)$$

the enthalpy change associated with reaction 1b is obtained from the slope of the van't Hoff plot while the entropy change is obtained from the intercept. At 284 K, the midpoint of the experimental 1/T range, this "second-law analysis" gives the results $\Delta H = -55.2 \pm 1.3$ kJ mol^{-1} and $\Delta S = -93.5 \pm 4.7$ J mol^{-1} K^{-1}, where the errors are 2σ and represent precision only.

CH_3ICl Thermochemistry: Third-Law Analysis. In addition to the second-law analysis described above, we have also carried out a third-law analysis, where the experimental value of K_p at 284 K, $(1.86 \pm 0.28) \times 10^5$ atm^{-1}, has been employed in conjunction with a calculated entropy change to determine ΔH.

Since experimental data concerning the structure of CH_3ICl are not available, ab initio calculations have been carried out for this species. The calculations employed the Gaussian 94 program.[45] Optimized geometries for CH_3I and CH_3ICl were

TABLE 3: Results of the $Cl(^2P_J) + CX_3I + N_2 \leftrightarrow CX_3ICl + N_2$ Equilibration Kinetics Experiments (X ≡ H or D)[a]

Cl + CH_3I

T	*P*	$[Cl_2]$	$[Cl]_{t=0}$	$[CH_3I]$	*Q*	$-\lambda_1$	$-\lambda_2$	k'_{1a}	k_3	k_5	k_{1b}	k_{-1b}	K_P
263	100	34	0.79	804	310	1270	56	37	57	45	11.5	265	1210
		34	0.79	1410	325	2190	54	66	57	43	12.7	281	1260
		34	0.79	2980	242	2950	60	139	57	51	8.63	192	1266
270	100	34	1.0	702	515	1260	58	37	36	48	10.4	467	607
		34	1.0	1490	542	2180	71	79	36	58	10.7	484	598
		34	1.0	3150	519	4130	65	166	36	47	11.0	472	634
		34	1.0	4490	449	5680	3	237	36	−22	11.1	471	639
		34	1.0	5540	500	6840	33	292	36	10	10.9	490	606
276	100	95	2.3	5020	949	6994	214	359	89	184	11.6	765	402
		95	2.7	5030	884	6630	198	360	89	166	10.9	718	405[b]
279	100	33	0.73	1620	973	2730	102	99	96	54	10.3	919	294
		33	0.73	4290	1090	6050	133	263	96	88	11.0	997	291
		33	0.73	5870	943	7540	86	359	96	35	10.6	909	307
283	100	34	1.0	1730	1290	3010	103	113	46	64	9.60	1230	203
		34	1.0	3570	1360	4870	134	233	46	81	9.44	1280	192
		34	1.0	5200	1290	6500	112	339	46	47	9.49	1240	198
		34	1.0	6580	1210	7970	82	429	46	12	9.67	1200	209
295	100	22	0.68	1180	2640	3380	125	92	44	88	6.16	2550	60.0
		22	0.75	1860	3360	5080	176	145	44	152	9.20	3200	71.4
		75	0.86	1890	3280	5160	179	148	44	157	9.86	3130	78.4
		22	0.73	2060	2990	4610	164	161	44	90	7.70	2900	66.2
		75	2.5	2200	3150	4830	202	172	44	177	7.56	2980	63.2
		5.5	0.18	2270	2750	4810	171	177	39	114	8.90	2630	84.1
		21	0.67	3570	2930	5890	205	279	44	92	7.98	2840	69.9
		5.5	0.18	4640	2810	7130	220	363	39	106	8.92	2700	82.1
		22	0.73	5090	2960	7410	234	398	44	101	8.35	2860	72.8
		22	0.67	5200	2960	7370	258	406	44	135	8.11	2820	71.5
		22	0.75	6670	3170	9490	308	521	44	186	9.09	2980	75.8
		77	1.5	7020	2880	9080	294	548	39	166	8.42	2710	77.3
		22	0.75	9990	3090	11300	327	780	44	149	7.76	2940	65.7
		22	0.74	12500	3190	14600	362	977	44	189	8.58	3010	71.1
		21	0.46	13700	2790	15600	271	1070	39	93	8.71	2700	80.3
		77	1.5	14000	3070	15800	398	1090	39	235	8.58	2840	75.2
		77	1.5	21000	2860	22000	301	1640	39	103	8.47	2760	76.4
		21	0.41	25000	3430	26700	619	1950	39	444	8.78	2990	73.1
297	250	53	1.6	3520	5380	10700	237	283	129	62	14.6	5310	67.9
		53	1.6	6690	5440	15400	306	538	129	114	14.4	5320	66.8
		53	1.6	10700	4970	21400	192	860	129	−53	14.6	5030	71.7
297	500	80	2.1	1260	7910	10800	290	101	137	426	23.2	7490	76.5
		70	2.0	1420	13200	17900	318	114	158	443	33.5	12700	65.1
		75	2.0	2160	6680	11000	323	174	137	341	20.1	6340	78.3
		71	2.0	2680	8290	13900	342	215	158	296	20.7	8000	64.0
		75	1.9	3490	7180	13900	377	281	137	335	19.0	6840	68.8
		70	2.0	4130	7670	16400	358	332	158	246	20.8	7420	69.3
300	25	27	0.60	6940	1630	4330	374	582	69	230	3.49	1400	61.1
		27	0.58	13700	1660	7230	404	1150	69	188	3.47	1480	57.5
		26	0.57	24100	1440	11100	360	2020	69	122	3.27	1320	60.5
309	100	43	1.1	4820	5650	8830	399	457	62	192	6.33	5460	27.6
		43	1.1	9590	6780	15400	584	908	62	294	8.60	6490	31.5
		43	1.1	15800	6090	18300	616	1500	62	158	7.14	5940	28.6
		43	1.1	21000	6430	23900	780	1990	62	337	7.71	6090	30.1

Cl + CD_3I

T	*P*	$[Cl_2]$	$[Cl]_{t=0}$	$[CH_3I]$	*Q*	$-\lambda_1$	$-\lambda_2$	k'_{4a}	k_3	k_9[c]	k_{4b}	k_{-4b}	K_P
298	100	18	1.4	1860	5160	8360	107	24	54	153	17.3	5010	85.1
		17	1.1	1920	5120	7580	10	25	54	−138	12.4	5260	58.2
		17	1.1	7560	4830	14950	10	99	54	−59	13.2	4890	66.5
		18	1.4	11000	4370	18400	7	145	54	−53	12.5	4430	69.3

[a] Units: *T*(K); *P*(Torr); concentrations(10^{11} cm^{-3}); *Q*, λ_1, λ_2, k_3, k_5, k'_{1a}, k_{-1b}(s^{-1}); k_{1b}(10^{-12} cm^3 $molecule^{-1}$ s^{-1}); K_P(10^3 atm^{-1}). [b] 1.1×10^{15} CF_2Cl_2 per cm^3 added as an additional $Cl(^2P_{1/2})$ quencher. [c] Reaction 9 is $CD_3ICl \rightarrow$ first-order loss by processes that do not regenerate Cl atoms.

determined using density functional theory[46−55] with the B3LYP exchange/correlation functional.[56] A 6-31+G(d) basis set was used for carbon and hydrogen, while an effective core potential (ECP)[57] was used for the core electrons of chlorine and iodine in conjunction with a 311/311/1 basis set contraction for the valence orbitals. This level of theory is denoted B3LYP/ECP.

Recently the G2[58a] and G2(MP2)[58b] levels of theory[59] have been extended to include iodine.[60] Both levels of theory approximate results from the QCISD(T)/6-311+G(3df,2p) level with zero-point and higher-order corrections. The computational method includes all electron calculations for carbon, hydrogen and chlorine, and either an all electron (AE) or an effective core potential (Hay-Wadt, ECP (HW), or Stuttgart, ECP (S)) for iodine. In the G2 computational scheme for iodine, a 11111/11111/1 contraction is used for the valence orbitals in place of the 6-311+G(d,p) basis set and a 11111/11111/111/1 contraction is used in place of the 6-311+G(3df,2p) basis set. The mean absolute deviations from experiment at the G2 [ECP (S)] level

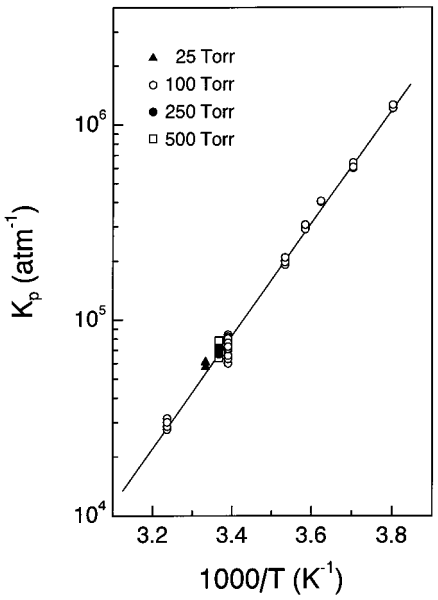

Figure 6. van't Hoff plot for the reaction Cl + CH_3I ↔ CH_3ICl. The solid line is obtained from a linear least-squares analysis and gives the second-law thermochemical parameters for the reaction (see Table 5). Different symbols indicate data obtained at different total pressures.

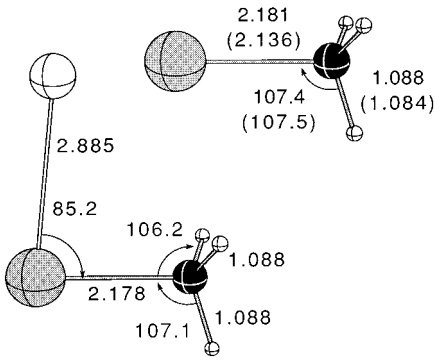

Figure 7. Structures for CH_3I and CH_3ICl derived from ab initio calculations at the Becke 3LYP/ECP level as discussed in the text. Bond lengths and bond angles shown in parentheses are experimental values taken from ref 63.

for iodine-containing molecules of ionization energies, electron affinities, and atomization energies is only 9.6 kJ/mol. Several applications of the G2 method to iodine-containing molecules have appeared.[61]

In this study we have followed the G2 [ECP (S)] prescription with the exception that we use B3LYP/ECP geometries and corresponding vibrational frequencies (with no scaling factor) rather than the MP2/ECP geometry and HF/ECP frequencies (with 0.893 scaling factor). Thus, we use the notation G2′ [ECP (S)] and G2′ (MP2) [ECP (S)] to denote this difference. Bauschlicher and Partridge have suggested similar modifications to the G2 scheme.[62]

The B3LYP/ECP calculated structures of CH_3I and CH_3ICl are shown in Figure 7. The calculated CH_3I structure is very similar to the structure obtained from microwave spectroscopy[63] (see Figure 7), thus providing some validation for the computational approach. The CH_3I-Cl adduct is characterized by a long Cl−I two-center three-electron (2c-3e) bond (2.886 Å) which is about 25% longer than a normal Cl−I 2c-2e bond to a divalent iodine[64] (ICl_2^+, 2.31 Å; $I_2Cl_2^+$, 2.34 Å). Upon complexing with a chlorine atom, the I−CH_3 bond contracts slightly (2.181 → 2.178 Å) while the methyl group adopts a staggered orientation with a pronounced tilt towards chlorine. That tilt in conjunction with the small Cl−I−C angle of 85.2° suggests a stabilizing hyperconjugative interaction[65] which is borne out by inspection of the population density where the empty π^* combination on CH_3 stabilizes an occupied out-of-plane lone pair orbital on chlorine.

TABLE 4: Summary of Parameters Used in Calculations of Absolute Entropies and Heat Capacity Corrections

	Cl	CH_3I	CH_3ICl
g_0	4	1	2
g_1	2		
$\Delta\epsilon$(cm^{-1})[a]	882.36		
σ		3	3[b]
I_{ABC}(amu^3 Å^6)[c]		1.48×10^4	5.03×10^6
I_r(amu Å^2)[d]			3.2
ν(cm^{-1})[e]		3060,[f] 2953, 1438[f] 1251, 883,[f] 533	3240, 3232, 3113 1475, 1481, 1303 920, 911, 501 171, 89, 19[g]

[a] $\Delta\epsilon \equiv$ Energy splitting between lowest two electronic states. CH_3I has no low-lying excited electronic states and CH_3ICl is assumed to have none. [b] Symmetry factor > 1 results from internal rotation of CH_3 about ICl. [c] I_{ABC} for CH_3I is based on experimental rotational constants. Using the calculated structure (Figure 7), we obtain $I_{ABC} = 1.58 \times 10^4$ amu^3 Å^6. [d] Moment of inertia for internal rotation of CH_3 about ICl. [e] Frequencies for CH_3I are based on experiment. Calculated frequencies in units of cm^{-1} are 3219,[f] 3106, 1490,[f] 1298, 896,[f] and 509. [f] Doubly degenerate vibrational modes. [g] This is the frequency for the internal rotation of CH_3 about ICl; this motion was treated as free rotation (see text), not a vibration.

TABLE 5: Thermochemical Parameters for the Reaction Cl(^2P_J) + CH_3I → CH_3ICl[a]

T	method	$-\Delta H$	$-\Delta S$
298	second law	55.2 ± 1.4	93.4 ± 4.8
	third law	52.0 ± 2.1	82.4 ± 6.0
284	second law	55.2 ± 1.3	93.5 ± 4.7
	third law	52.0 ± 1.3	82.3 ± 6.0
0	second law	53.7 ± 1.5	
	third law	50.6 ± 2.2	

[a] Units: T(K); ΔH(kJ mol^{-1}); ΔS(J mol^{-1} K^{-1}). [b] Errors are 95%-confidence-level estimates.

To carry out the third-law analysis, absolute entropies as a function of temperature were obtained from the JANAF tables[66] for Cl, calculated using vibrational frequencies and rotational constants taken from the literature[67] for CH_3I, and calculated using ab initio vibrational frequencies and moments of inertia for CH_3ICl. The lowest frequency normal mode for CH_3ICl (with $\tilde{\nu} = 19$ cm^{-1}) is the internal rotation of the methyl group around ICl. Some additional calculations, carried out to assess the magnitude of the barrier to internal rotation, suggest that the barrier is very small (i.e., 0.75 kJ mol^{-1}); hence, in the third law calculations the lowest frequency normal mode of CH_3ICl was treated as a free rotation. At 284 K, the third law analysis gives the results $\Delta H = -52.0 \pm 1.3$ kJ mol^{-1} and $\Delta S = -82.3 \pm 6.0$ J mol^{-1} K^{-1}; the uncertainties we report reflect an estimate of our imperfect knowledge of the input data needed to calculate absolute entropies (the low-frequency vibrations of CH_3ICl are most significant) as well as the estimated uncertainty in the experimental value for K_p(284 K).

Summary of Thermochemical Results. The thermochemical results of this study are summarized in Table 5. Appropriate heat capacity corrections have been employed to obtain ΔH values at 298 and 0 K. Using literature values[66,68] for the heats of formation of Cl and CH_3I at 298 and 0 K allows the heat of formation of CH_3ICl to be evaluated. As can be seen from Table 5, the agreement between the second- and third-law results, while not perfect, is pretty good. Since the uncertainties in the $\Delta H_{f,T}(CH_3ICl)$ values obtained by the two methods are similar in magnitude, it seems appropriate to report simple

averages of the second- and third-law values, while adjusting reported uncertainties to encompass the 2σ error limits of both determinations. Using this approach, we report $\Delta H^\circ_{f,298}(CH_3ICl) = 82.3 \pm 3.5$ kJ mol^{-1} and $\Delta H^\circ_{f,0}(CH_3ICl) = 91.6 \pm 3.6$ kJ mol^{-1}.

For comparison with the experimental values for the CH_3I-Cl bond strength (see ΔH values in Table 5), theoretical values have been obtained using density functional theory (DFT) at the B3LYP/ECP level, and also using G2 and G2(MP2) theories (see above). Calculated values for $-\Delta H$ at 0 K are as follows:

B3LYP/ECP	59.3 kJ mol^{-1}
G2′ (MP2) [ECP(S)]	42.5 kJ mol^{-1}
G2′ [ECP(S)]	40.0 kJ mol^{-1}

The theoretical bond strengths bracket the experimental value of 52 ± 3 kJ mol^{-1} (average of second- and third-law determinations), with density functional theory predicting a stronger bond than observation and the G2 theories predicting a weaker bond. Overall, however, the agreement between theory and experiment is reasonably good.

Comparison with Previous Research. The only experimental study of $Cl + CH_3I$ kinetics reported in the literature was published very recently by Kambanis et al.[29] These authors used the very low-pressure reactor technique to study reaction 1 at millitorr pressures over the temperature range 273−363 K; they report the Arrhenius expression $k_1 = (1.33 \pm 0.49) \times 10^{-11} \exp[(-689 \pm 120)/T]$ cm^3 molecule^{-1} s^{-1}. Because of the low pressures employed by Kambanis et al., the dominant reaction channel under their experimental conditions is probably hydrogen transfer, i.e., reaction 1a. Comparison with our Arrhenius expression for $k_{1a}(= 5.44 \times 10^{-11} \exp(-1250/T)]$ shows good agreement with the results of Kambanis et al. at $T \sim 363$ K but not very good agreement at $T \sim 273$ K, where the rate coefficient obtained from our expression (which admittedly is based entirely on high-temperature data) is a factor of 2 slower than the rate coefficient reported by Kambanis et al. One disturbing aspect of the comparison of Kambanis et al.'s results with ours concerns observed kinetic isotope effects—they find $k_1/k_4 = 1.09 \pm 0.04$ independent of temperature over the range 273−363 K, while we find $k_1/k_4 = 4.3$ at 373 K and $k_1/k_4 = 3.6$ at 419 K; the reason for this significant discrepancy is not clear.

In addition to the experimental study discussed above, Lazarou et al.[30] have recently reported ab initio calculations of the CH_3ICl structure and bond strength at the MP2/3-21++G-(2d,2p) level of theory; their structure is very similar to the structure reported in this paper, and their calculated 0 K bond dissociation energy of 50.7 kJ mol^{-1} is essentially in perfect agreement with the experimental value reported in this paper.

The first indication that Cl reactions with iodoalkanes may involve a complex mechanism came from product angular distributions observed in molecular beam studies by Hoffmann et al.[69,70] In addition to reaction 1, we have recently observed reversible adduct formation in reactions of Cl with CH_3Br, CF_3I, CF_3CH_2I, and CD_3CD_2I.[31] Ab initio calculations predict 298 K bond strengths similar to those which were measured (ranging from 24.5 kJ mol^{-1} for CH_3Br-Cl to 59.1 kJ mol^{-1} for CD_3-CD_2I-Cl). Both experiment and theory show an excellent inverse correlation between the adduct bond strength and the haloalkane ionization potential.[31] Evidence for complex formation has also been observed in a recent study of the reaction of Cl with CH_2ClI.[71] The $Cl + CH_2ClI$ reaction behaves differently from the reactions discussed above, however, in that dissociation of the adduct back to reactants is not observed; in this case, adduct dissociation to $CH_2Cl + ICl$ is energetically favorable, whereas the dihalogen dissociation channel is energetically unfavorable for other reactions studied to date.

Implications for Atmospheric Chemistry. The dominant established CH_3I destruction process in the atmosphere is photolysis. Recent evaluations of the atmospheric CH_3I photolysis rate coefficient[11,12] suggest that a value of about 5×10^{-6} s^{-1} is typical for the tropical and midlatitude marine boundary layer (MBL). Chlorine atom levels in the MBL are rather poorly established, but the best available estimates suggest concentrations of about 10^4 per cm^3; using this estimate in conjunction with the value $k_1 \sim 2.5 \times 10^{-11}$ cm^3 molecule^{-1} s^{-1} (see Tables 2 and 3) under typical MBL conditions of temperature and pressure, gives a pseudo-first-order rate coefficient of 2.5×10^{-7} s^{-1} for CH_3I destruction by Cl atoms if addition of Cl to CH_3I is completely irreversible under atmospheric conditions. Hence, reaction 1 will compete with photolysis as an atmospheric destruction mechanism for CH_3I only if (a) the average marine boundary layer concentration of Cl atoms is near the high end of the range of possible values and (b) the fate of CH_3ICl under atmospheric conditions is not dissociation back to $Cl + CH_3I$. Even though it appears unlikely that reaction 1 is an important removal mechanism for atmospheric CH_3I, its potential role in atmospheric chemistry cannot be completely understood until the fate of CH_3ICl under atmospheric conditions is established. For example, there is some indication that CH_3ICl can isomerize, then dissociate to give $CH_3Cl + I$,[72,73] although our results suggest that dissociation to $CH_3I + Cl$ is the predominant unimolecular CH_3ICl loss process, i.e., $k_{-1b} \gg k_5$ (see Table 3).

Acknowledgment. The experimental component of this research was supported by the National Aeronautics and Space Administration, Upper Atmosphere Research Program, through grants NAGW-1001 and NAG5-3634 to Georgia Institute of Technology. Computer time for this study was made available by the Alabama Supercomputer Network.

References and Notes

(1) Liss, P. S.; Slater, P. G. *Nature* **1974**, *247*, 181.
(2) Rasmussen, R. A.; Khalil, M. A. K.; Gunawardena, R.; Hoyt, S. D. *J. Geophys. Res.* **1982**, *87*, 3090.
(3) Singh, H. B.; Salas, L. J.; Stiles, R. E. *J. Geophys. Res.* **1983**, *88*, 3684.
(4) Reifenhauser, W.; Heumann, K. G. *Atmos. Environ.* **1992**, *26A*, 2905.
(5) Oram, D. E.; Penkett, S. A. *Atmos. Environ.* **1994**, *28*, 1159.
(6) Davis, D.; Crawford, J.; Liu, S.; McKeen, S.; Bandy, A.; Thornton, D.; Rowland, F.; Blake, D. *J. Geophys. Res.* **1996**, *101*, 2135.
(7) Chameides, W. L.; Davis, D. D. *J. Geophys. Res.* **1980**, *85*, 7383.
(8) Jenkin, M. E.; Cox, A. R.; Candeland, D. E. J. Atmos. Chem. **1985**, *2*, 359.
(9) Chatfield, R. B.; Crutzen, P. J. *J. Geophys. Res.* **1990**, *95*, 22319.
(10) Solomon, S.; Garcia, R. R.; Ravishankara, A. R. *J. Geophys. Res.* **1994**, *99*, 20491.
(11) Roehl, C. M.; Burkholder, J. B.; Moortgat, G. K.; Ravishankara, A. R.; Crutzen, P. J. *J. Geophys. Res.* **1997**, *102*, 12819.
(12) Rattigan, O. V.; Shallcross, D. E.; Cox, R. A. *J. Chem. Soc., Faraday Trans.* **1997**, *93*, 2839.
(13) Garraway, J.; Donovan, R. J. *J. Chem. Soc., Chem. Commun.* **1979**, 1108.
(14) Brown, A. C.; Canosa-Mas, C. E.; Wayne, R. P. *Atmos. Environ.* **1990**, 24A, 361.
(15) See, for example: Crutzen, P. J. In *Composition, Chemistry, and Climate of the Atmosphere*; Singh, H. B., Ed.; Van Nostrand Reinhold: New York, 1995; pp 349−393.
(16) Jobson, B. T.; Niki, H.; Yokouchi, Y.; Bottenheim, J.; Hopper, F.; Leaitch, R. *J. Geophys. Res.* **1994**, *99*, 25355.
(17) Singh, H. B.; Gregory, G. L.; Anderson, B.; Browell, E.; Sachse, G. W.; Davis, D. D.; Crawford, J.; Bradshaw, J. D.; Talbot, R.; Blake, D. R.; Thornton, D.; Newell, R.; Merrill, J. *J. Geophys. Res.* **1996**, *101*, 1907.
(18) Singh, H. B.; Thakur, A. N.; Chen, Y. E. *Geophys. Res. Lett.* **1996**, *23*, 1529.
(19) Vogt, R.; Crutzen, P. J.; Sander, R. *Nature* **1996**, *383*, 327.

(20) Finlayson-Pitts, B. *J. Res. Chem. Intermed.* **1993**, *19*, 235.
(21) Manning, R. G.; Kurylo, M. J. *J. Phys. Chem.* **1977**, *81*, 291.
(22) Tschuikow-Roux, E.; Yano, T.; Niedzielski, J. *J. Chem. Phys.* **1985**, *82*, 62.
(23) Tuazon, E. C.; Atkinson, R.; Corchnoy, S. B. *Int. J. Chem. Kinet.* **1992**, *24*, 639.
(24) Wallington, T. J.; Ball, J. C.; Nielsen, O. J.; Bartkiewicz, E. *J. Phys. Chem.* **1992**, *96*, 1241.
(25) Clyne, M. A. A.; Walker, R. F. *J. Chem. Soc., Faraday Trans. 1* **1973**, *69*, 1547.
(26) Wallington, T. J.; Andino, J. M.; Ball, J. C.; Japar, S. M. J. *Atmos. Chem.* **1990**, *10*, 301.
(27) Tschuikow-Roux, E.; Faraji, F.; Paddison, S.; Niedzielski, J.; Miyokawa, K. *J. Phys. Chem.* **1988**, *92*, 1488.
(28) Gierczak, T.; Goldfarb, L.; Sueper, D.; Ravishankara, A. R. *Int. J. Chem. Kinet.* **1994**, *26*, 719.
(29) Kambanis, K. G.; Lazarou, Y. G.; Papagiannakopoulos, P. *Chem. Phys. Lett.* **1997**, *268*, 498.
(30) Lazarou, Y. G.; Kambanis, K. G.; Papagiannakopoulos, P. *Chem. Phys. Lett.* **1997**, *271*, 280.
(31) Piety, C. A.; Nicovich, J. M.; Ayhens, Y. V.; Estupinan, E. G.; Soller, R.; McKee, M. L.; Wine, P. H. 14th International Symposium on Gas Kinetics, Leeds, U.K., 1996; Abstract D6.
(32) Stickel, R. E.; Nicovich, J. M.; Wang, S.; Zhao, Z.; Wine, P. H. *J. Phys. Chem.* **1992**, *96*, 9875 and references therein.
(33) Nicovich, J. M.; Wang, S.; Wine, P. H. *Int. J. Chem. Kinet.* **1991**, *27*, 359.
(34) Nicovich, J. M.; Wang. S.; McKee, M. L.; Wine, P. H. *J. Phys. Chem.* **1996**, *100*, 680.
(35) Waschewsky, G. C. G.; Horansky, R.; Vaida, V. *J. Phys. Chem.* **1996**, *100*, 11559 and references therein.
(36) Stated minimum purity of liquid phase in high-pressure cylinder.
(37) Busch, G. E.; Mahoney, R. T.; Morse, R. I.; Wilson, K. R. *J. Chem. Phys.* **1969**, *51*, 449.
(38) Park, J.; Lee Y.; Flynn, G. W. *Chem. Phys. Lett.* **1991**, *186*, 441.
(39) Tyndall, G. S.; Orlando, J. J.; Kegley-Owen, C. S. *J. Chem. Soc., Faraday Trans.* **1995**, *91*, 3055.
(40) Fletcher, I. S.; Husain, D. *Chem. Phys. Lett.* **1977**, *49*, 516.
(41) Clark, R. H.; Husain, D. *J. Photochem.* **1983**, *21*, 93.
(42) Chichinin, A. I.; Krasnoperov, L. N. *Chem. Phys. Lett.* **1989**, *160*, 448.
(43) See for example, DeMore, W. B.; Sander, S. P.; Golden, D. M.; Hampson, R. F.; Kurylo, M. J.; Howard, C. J.; Ravishankara, A. R.; Kolb, C. E.; Molina, M. J. Chemical Kinetics and Photochemical Data for Use in Stratospheric Modeling; Evaluation No. 12, Jet Propulsion Laboratory Publication 97-4, 1997.
(44) Seetula, J. A.; Gutman, D.; Lightfoot, P. D.; Rayez, M. T.; Senkan, S. M. *J. Phys. Chem.* **1991**, *95*, 10688.
(45) Frisch, J. J.; Trucks, G. W.; Schlegel, H. B.; Gill, P. M. W.; Johnson, B. G.; Robb, M. A.; Cheeseman, J. R.; Keith, T.; Petersson, G. A.; Montgomery, J. A.; Raghavachari, K.; Al-Laham, M. A.; Zakrzewski, V. G.; Ortiz, J. V.; Foresman, J. B.; Cioslowski, J.; Stefanov, B. B.; Nanayakkara, A.; Challacombe, M.; Peng. C. Y.; Ayala, P. Y.; Chen, W.: Wong, M. W.; Andres, J. L.; Replogle, E. S.; Gomperts, R.; Martin, R. L.; Fox, D. J.; Binkley, J. S.; Defrees, D. J.; Baker, J.; Stewart, J. P.; Head-Gordon, M.; Gonzalez, C.; Pople, J. A. *Gaussian 94* (Rev. B.1); Gaussian, Inc.: Pittsburgh, PA, 1995.
(46) Bartolotti, L. J.; Flurchick, K. *An Introduction to Density Functional Theory*; In Reviews in Computational Chemistry 7; Lipkowitz, K. B., Boyd, D. B., Eds.; VCH: New York, 1996.
(47) Parr, R. G.; Yang, W. *Density-Functional Theory of Atoms and Molecules*; Oxford Press: Oxford, 1989.
(48) Ziegler, T. *Chem. Rev.* **1991**, *91*, 651.
(49) *Density Functional Methods in Chemistry*; Labanowski, J. K., Andzelm, J. W., Eds.; Springer: Berlin, 1991.
(50) Johnson, B. G.; Gill, P. M. W.; Pople, J. A. *J. Chem. Phys.* **1993**, *98*, 5612.
(51) Gill, P. M. W.; Johnson, B. G.; Pople, J. A., Frisch, M. *J. Chem. Phys. Lett.* **1992**, *197*, 499.
(52) Raghavachari, K.; Strout, D. L.; Odom, G. K.; Scuseria, G. E.; Pople, J. A.; Johnson, B. G.; Gill, P. M. W. *Chem. Phys. Lett.* **1993**, *214*, 357.
(53) Raghavachari, K.; Zhang, B.; Pople, J. A.; Johnson, B. G.; Gill, P. M. W. *Chem. Phys. Lett.* **1994**, *220*, 1994.
(54) Johnson, B. G.; Gonzales, C. A.; Gill, P. M. W.; Pople, J. A. *Chem. Phys. Lett.* **1994**, *221*, 100.
(55) Baker, J.; Scheiner, A.: Andzelm, J. *Chem. Phys. Lett.* **1993**, *216*, 380.
(56) Becke, A. D. *J. Chem. Phys.* **1993**, *98*, 5648.
(57) (a) Bergner, A.; Dolg, M.; Küchle, W.; Stoll, H.; Preuss, H. *Mol. Phys.* **1993**, *80*, 1431. (b) Schwerdtfeger, P.; Dolg, M.; Schwarz, W. H.; Bowmaker, G. A.; Boyd, P. D. W. *J. Chem. Phys.* **1989**, *91*, 1762.
(58) (a) Curtiss, L. A.; Raghavachari, K.; Trucks, G. W.; Pople, J. A. *J. Chem. Phys.* **1991**, *94*, 7221. (b) Curtiss, L. A.; Raghavachari, K.; Pople, J. A. *J. Chem. Phys.* **1993**, *98*, 1293.
(59) (a) Curtiss, L. A.; Raghavachari, K.; Trucks, G. W. In *Quantum Mechanical Electronic Structure Calculations with Chemical Accuracy*; Langhoff, S. R., Ed.; Kluwer Academic: Netherlands, 1995. (b) Raghavachari, K.; Curtiss, L. A. In *Modern Electronic Structure Theory*; Yarkony, D. R., Ed.; World Scientific: Singapore, 1995.
(60) Glukhovtsev, N. M.; Pross, A.; McGrath, M. P.; Radom, L. *J. Chem. Phys.* **1995**, *103*, 1878; Erratum: *J. Chem. Phys.* **1996**, *104*, 3407.
(61) (a) Glukhovtsev, M. N.; Pross, A.; Radom, L. *J. Am. Chem. Soc.* **1995**, *117*, 9012. (b) Glukhovtsev, M. N.; Pross, A.; Radom, L. *J. Phys. Chem.* **1996**, *100*, 3498. (c) Glukhovtsev, M.; Bach, R. D. *Chem. Phys. Lett.* **1997**, *269*, 145.
(62) (a) Baushlicher, C. W., Jr.; Partridge, H. *J. Chem. Phys.* **1995**, *103*, 1788. (b) Curtiss, LA.; Raghavachari, K.; Redfern, P. C.; Pope, J. A. *Chem. Phys. Lett.* **1997**, *270*, 419.
(63) *Structure of Free Polyatomic Molecules, Landolt-Börnstein, New Series*; Madelung, O., Ed.; Springer-Verlag: New York, 1987; Vol. 15.
(64) Cotton, F. A.; Wilkinson, G. *Advanced Inorganic Chemistry*, 5th ed.; Wiley: New York, 1988; p 577.
(65) Radom, L. *Structural Consequences of Hyperconjugation in Molecular Structure and Conformation*; Czismadia, I. G., Ed.; Elsevier: New York, 1982; pp 1−64.
(66) Chase, M. W., Jr.; Davies, C. A.; Downey, J. R., Jr.; Frurip, D. J.; McDonald, R. A.; Syverud, A. N. *J. Phys. Chem. Ref. Data* **1985**, *14* (Suppl. I).
(67) Herzberg, G. H. *Electronic Spectra of Polyatomic Molecules*; Van Nostrand Reinhold: New York, 1966.
(68) Atkinson, R.; Baulch, D. L.; Cox, R. A.; Hampson, R. F.; Kerr, J. A.; Troe, J. *J. Phys. Chem. Ref. Data* **1992**, *21*, 1125.
(69) Hoffmann, S. M. A.; Smith, D. J.; Gonzalez Urena, A.; Steele, T. A.; Grice, R. *Mol. Phys.* **1984**, *53*, 1067.
(70) Hoffmann, S. M. A.; Smith, D. J.; Gonzalez Urena, A.; Steele, T. A.; Grice, R. *Chem. Phys. Lett.* **1984**, *107*, 99.
(71) Bilde, M.; Sehested, J.; Nielsen, O. J.; Wallington, T. J.; Meagher, R. J.; McIntosh, M. E.; Piety, C. A.; Nicovich, J. M.; Wine, P. H. *J. Phys. Chem. A* **1997**, *101*, 8035.
(72) Bilde, M.; Wallington, T. J. *J. Phys. Chem. A*, submitted.
(73) (a) Goliff, W. Dissertation, University of California−Irvine, 1997. (b) Goliff, W.; Rowland, F. S. To be published.